Kirkland, C.L., et al., 2022, Did transit through the galactic spiral arms seed crust production on the early Earth?: Geology, v. 50, https://doi.org/10.1130/G50513.1

Supplemental Material

Did transit through the galactic spiral arms seed crust production on the early Earth?

Christopher L. Kirkland[1], Phil J. Sutton[2], Timmons M. Erickson[3], Tim E. Johnson[1], Michael Hartnady[1], Hugh Smithies[1,4], Mike Prause[4]

[1]Timescales of Mineral Systems Group, School of Earth and Planetary Science, Curtin University; Perth, Western Australia, Australia
[2]University of Lincoln, School of Mathematics and Physics; Brayford Pool, Lincoln, LN6 7TS, United Kingdom
[3]Jacobs—JETS, Astromaterials Research and Exploration Science Division, NASA Johnson Space Center; 2101 NASA Parkway, Houston, TX, 77058, USA
[4]Geological Survey of Western Australia, Department of Mines, Industry Regulation and Safety; Perth, Western Australia, Australia

Corresponding author: Christopher Kirkland. Building 312, School of Earth and Planetary Science, Curtin University, Perth, Western Australia, Tel. 08926664956

Corresponding author: c.kirkland@curtin.edu.au

Materials

New zircon laser ablation inductively coupled plasma mass spectrometry Hf isotope analyses were performed on 28 samples from the North Atlantic Craton (NAC), and addition zircon Hf data is from Gardiner et al., (2017), Gardiner et al., (2016), Gardiner et al., (2021), Gardiner et al., (2019), Kemp et al., (2015), Kirkland et al., (2018), Petersson et al., (2020), Petersson et al., (2019a), and Petersson et al., (2019b). All tabulated data used in this manuscript is included in DR2. Sample details for the new NAC samples are given in DR2, table 1. Sample details for the Pilbara Craton samples are provided in GSWA, (2020). Average $^{207}Pb/^{206}Pb$ age uncertainty for dated zircon is 27 Ma.

New Hf analyses of previously dated magmatic zircon grains from the NAC are combined with published zircon Hf data from the NAC to produce an isotopic time series that is evaluated for its frequency components. Newly acquired NAC zircon Hf isotopic data are provided in DR2, table 1 and the NAC time series in DR2, table 2. Zircon U-Pb geochronology for all NAC samples is given in Olierook et al., (2021). Pilbara Craton zircon Hf isotope data are compiled from Gardiner et al., (2017), Gardiner et al., (2021), Gardiner et al., (2019), Kemp et al., (2015), Petersson et al., (2020), Petersson et al., (2019a), Petersson et al., (2019b). The Pilbara Craton zircon Hf isotope time series is supplied in DR2, table 3. Measured Hf isotopic values of reference zircon are given in DR2, table 4.

A compilation of oxygen isotope and accompanying U-Pb age data from Smithies et al., (2021) and Johnson et al., (2022) for Pilbara Craton zircon crystals is provided in DR2,

table 5 and is also available through the public geoscience repository "Geoview" at http://www.dmp.wa.gov.au/geochron/ see Lu et al., (2021). Extended U-Pb data tables for all investigated NAC and Pilbara samples are available in Geological Survey of Western Australia, (2020) and Olierook et al., (2021).

Data Preparation and Spectral Analysis

Quantiles at the 25th, 50th, and 75th level were fitted to the NAC and Pilbara zircon Hf timeseries using the 'zoo'(Zeileis and Grothendieck, 2005) package in R on a 25 Ma moving bin. The 50th fit of the timeseries is used in spectral analysis with a REDFIT procedure from Schulz and Mudelsee, (2002). Overlapped segment averaging (with 50% overlap) is employed, to reduced noise, using a two-segment average. Timeseries of the 25th, 50th, and 75th quantiles for both NAC and Pilbara datasets are given in DR2; table 2 and 3, for the NAC and Pilbara cratons, respectively. Additionally, a continuous wavelet transform (Torrence and Compo, 1998) as implemented in Past4 (Hammer et al., 2001) is applied to the various quantiles, with a Morlet mother wavelet.

Analytical Method; Lu-Hf Analysis

New NAC zircon Lu-Hf samples were analyzed by laser ablation multi-collector inductively coupled plasma mass spectrometry (LA-MCICPMS) at the John de Laeter Centre, Curtin University. Zircon grains were ablated using a Resonetics RESOlution M-50A-LR sampling system (incorporating a Compex 102 excimer laser) coupled to a Nu Plasma II MC-ICP-MS. Following 15-20 seconds of background analysis, samples were ablated for 30 seconds at a 7 Hz repetition rate using either a 33 or 50 µm beam spot, dependent on grain size, and laser energy of 1.5 J/cm^2. The sample cell was flushed by ultrahigh purity He (0.68 L min^{-1}) and N_2 (2.8 mL min^{-1}). High purity Ar was used as the plasma gas (flow rate 0.98 L min^{-1}). During time-resolved processing, contamination resulting from inclusions and compositional zoning was monitored, and only the relevant part of the signal integrated.

Measurements of ^{171}Yb, ^{172}Yb, ^{173}Yb, ^{175}Lu, ^{176}Hf + Yb + Lu, ^{177}Hf, ^{178}Hf, ^{179}Hf, and ^{180}Hf were made simultaneously. Time-resolved data were baseline subtracted and reduced using an Iolite data reduction scheme after ref. (Woodhead et al., 2004), where ^{176}Yb and ^{176}Lu were removed from the 176 mass signal using ^{176}Yb/^{173}Yb = 0.7962 and ^{176}Lu/^{175}Lu = 0.02655 with an exponential law mass bias correction assuming ^{172}Yb/^{173}Yb = 1.3527457. The interference corrected ^{176}Hf/^{177}Hf was normalized assuming ^{179}Hf/^{177}Hf = 0.732558 for mass bias correction. Mud Tank zircon was used as the primary reference material for Hf isotope ratios, with a ^{176}Hf/^{177}Hf ratio of 0.282507 ± 0.00000659. Zircon 91500 (0.282305 ± 0.000006; Blichert-Toft, 2008), GJ-1 (0.282000 ± 0.000005; Morel et al., 2008), and FC1 (0.282183 ± 0.000012; Fisher et al., 2014) were used as secondary reference material to monitor data accuracy. During these analyses secondary reference zircon had mean values within two standard deviations of the accepted ^{176}Hf/^{177}Hf value (DR2, table 4), including 91500 (0.282282 ± 0.000032), GJ-1 (0.282003 ± 0.000021), and FC1 (0.282162 ± 0.000036). The stable ^{180}Hf/^{177}Hf ratio for all unknown analyses yielded a weighted mean value of 1.886849 ± 0.000010 (n =

466 of 494; MSWD = 1.8), which overlaps with recommended values (Thirlwall and Anczkiewicz, 2004). Decay constants, chondritic uniform reservoir (CHUR), and depleted mantle values are taken from Söderlund et al., (2004), Bouvier et al., (2008), and Griffin et al., (2002b), respectively. Epsilon notation Hf isotopic data relative to CHUR at the initial time of crystallization (εHf_i) were computed for concordant zircon grains using the age of the crystal, and the measured (present-day) $^{176}Lu/^{177}Hf$ and $^{176}Hf/^{177}Hf$ values.

Spectral Analysis

To facilitate further comparison of the NAC and Pilbara zircon Hf timeseries, the Mesoarchaean and older (>3200 Ma) segment of the NAC data set is subject to further wavelet analysis using the approach of Foster, (1996) suitable for unequal sample spacing of the original zircon analyses. Wavelet analysis of this >3200 Ma segment of the North Atlantic Craton zircon Hf data set (DR2, table 2) reveals a continuous frequency band at ~170 Myr (Ma^{-1}) as well as a long period frequency at ~250 Myr and a discontinuous shorter frequency at ~74 Myr (Supplemental Fig. S1). The ~250 Myr frequency is within the zone of edges effects. Nonetheless, the ~170 Myr frequency is outside the zone of edge effects and a similar frequency to that within the Pilbara Craton zircon Hf timeseries.

Pilbara Magmatic Zircon Hf Crustal Residence Age and Oxygen Isotopes

Zircon oxygen isotope values from the eastern Pilbara are collated from Smithies et al., (2021) and Johnson et al., (2022) (see DR2, table 5) and further details on the instrument parameters and secondary reference zircon values are provided in those works. $^{18}O/^{16}O$ ratios and $^{16}O^{1}H/^{16}O$ (OH^-), were determined simultaneously on a Cameca IMS 1280 for most analyses reported in this compilation. Analyses have on average an internal precision of 0.2‰ (2 SD mean). Drift corrected $^{18}O/^{16}O$ ratios are reported in $\delta^{18}O$ notation, in per mil variations relative to VSMOW. Analyses are filtered for U-Pb concordance, with only data >95% concordant used for further timeseries analysis. $^{16}O^{1}H/^{16}O$ values are also used to qualitatively assess if the zircon oxygen isotopic values reflect a primary signature (Pidgeon et al., 2013). The level for the $^{16}O^{1}H/^{16}O$ filter is set at the maximum $^{16}O^{1}H/^{16}O$ measured from the crystalline reference material run in the same analytical session, on the same sample mount, as the unknown. Analyses with $^{16}O^{1}H/^{16}O$ values higher than this filter are regarded as secondary and not considered further. Primary magmatic zircon $\delta^{18}O$ values over time have a LOWESS curve fitted to them (LOcally Weighted Scatterplot Smoothing, Cleveland, 1979) with bootstrapped 95% confidence band calculated using 999 random replicates.

Zircon crustal residence ages (DR2, table 6) were calculated from the same Pilbara zircon compilation as the Hf time series (DR2, table 3). The crustal residence time series is based on a regular 25 Ma interpolation of the LOWESS fit to zircon Hf two stage depleted mantle model age minus $^{207}Pb/^{206}Pb$ zircon crystallization age. This value (in Ma) reflects an estimate of the average length of time that the source components, for the melt that the zircon crystallized from, resided within the crust. Calculation of model ages (T_{DM}^2) are based on a depleted-mantle source with $^{176}Hf/^{177}Hf_i = 0.279718$ at 4.56 Ga and

$^{176}Lu/^{177}Hf = 0.0384$ (Griffin et al., 2000). Each two-stage model age assumes that Hf resided within a parental source with average $^{176}Lu/^{177}Hf$ of 0.015 (Griffin et al., 2002a), prior to incorporation within the zircon. Spherule bed ages follow that compiled in Glikson and Pirajno (2018).

Milky Way Relative Mass Density Model

Relative mass density profiles for spiral galaxies relate to the distribution of mass over the radial and azimuthal directions. Radial profiles typically show a reduction in surface densities with increasing distance from the galactic center (Sanchez-Blazquez et al., 2009). The density profiles as a function of azimuthal angle, which is in the direction of the galactic plane, vary with angle due to the spiral arm pattern (Junqueira et al., 2013). Peak densities in the azimuth direction occur at the mid-points of the spiral arms with minimum densities located in the areas separating spiral arms. Close to the center of the galaxy the azimuth profile resembles a sine wave, with mass density peaks occurring near the middle of the spiral arm and troughs at the mid-point between arms. As the radial distance increases the azimuthal profile becomes flatter when outside the spiral arms. Physically, this means that mass is more evenly distributed outside the spiral arms as distance increases from the galactic center (Junqueira et al., 2013). Given the Sun is located at around 8 Kpc from the galactic center, we create an azimuthal density profile that assumes the largest local densities occur at the center of the spiral arms with a normal distribution. The density profile outside the arms is taken to be at a minimum and to remain constant until approach of the next arm. Despite commonly depicted as having two major arms (Scutum–Crux–Centaurus & Perseus) and two minor arms (Sagittarius–Carina & Norma), all four arms of the Milky Way are considered to have similar widths (Vallée, 2017). Therefore, we adopt the time taken to pass through each arm of 63 Myr, similar to values identified via extinctions events in the fossil record (62 ± 3 Myr) (Lieberman and Melott, 2007; Melott and Bambach, 2011; Rohde and Muller, 2005) and estimated from galactic structure models (63.4 Myr) (Gillman and Erenler, 2019) (DR2, table 7).

Model assumptions:

- Average time to pass through a spiral arm is 63 Myr.
- Each arm is the same width.
- Arms are evenly spaced between one another.
- Orbital velocity does not change. However, where density waves cause the spiral arm structure it is expected that stars vary their orbital velocity as they pass through and out of the arms.
- Pitch angle of the spiral arms does not evolve through time. This would not change the period of arm passage. Instead it would alter the time in the spiral arms as the Solar System passes through at swallower angle.

Code availability

Iolite used for zircon LA-ICPMS Hf data reduction is available through https://iolite.xyz/. Past4 used for spectra analysis is available through https://www.nhm.uio.no/english/research/infrastructure/past/

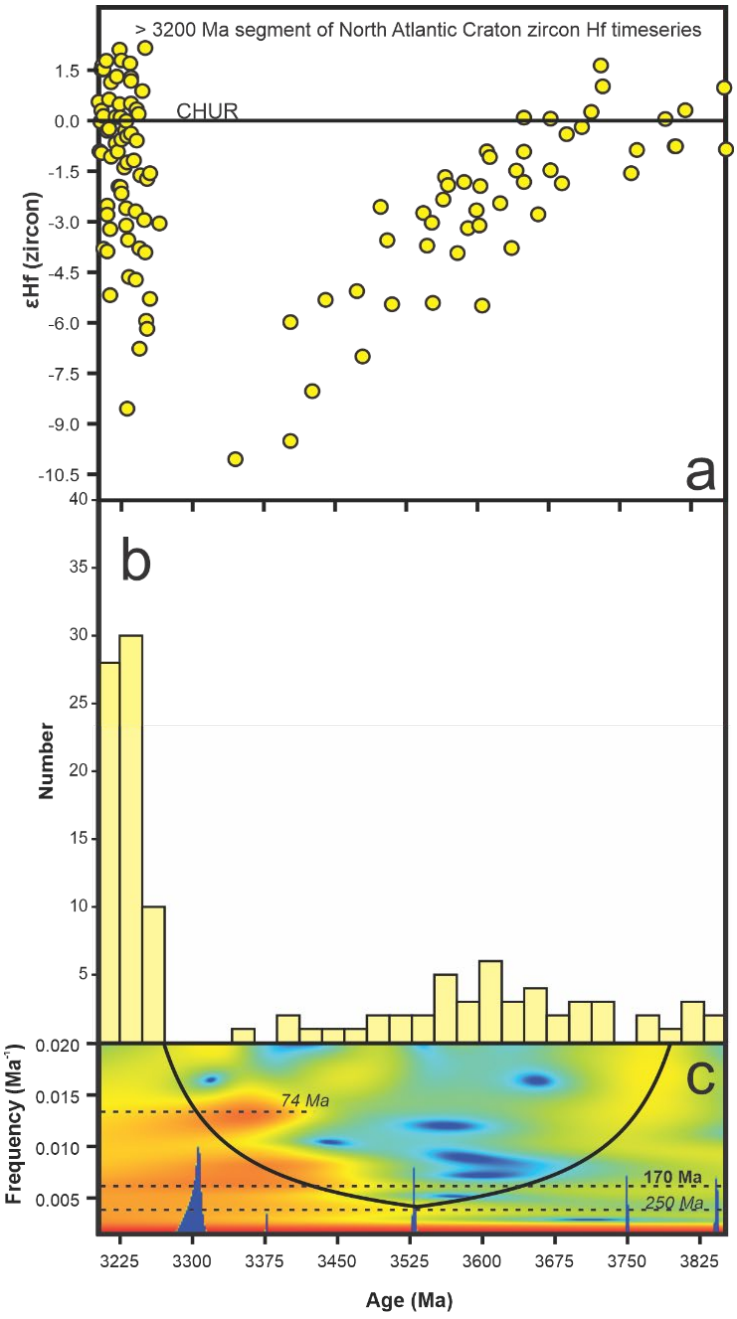

Supplemental Figure S1: Wavelet analysis of the >3200 Ma (Million Year) segment of the North Atlantic Craton zircon Hf dataset (DR2, table 1) (a) Zircon Hf evolution plot

with chondritic uniform reservoir shown as sold black line; CHUR values: $^{176}Lu/^{177}Hf$ = 0.0336, $^{176}Hf/^{177}Hf$ = 0.282785 (Bouvier et al., 2008) and $\lambda^{176}Lu = 1.867\times10^{-11}$a (Söderlund et al., 2004). (b) Histogram of number of zircon Hf analyses. (c) Wavelet analysis based on the weighted wavelet z transform, which evaluates unevenly spaced samples (see supplementary note in Table S1).

References

Blichert-Toft, J., 2008, The Hf isotopic composition of zircon reference material 91500. : Chemical Geology, v. 253, p. 252-257.

Bouvier, A., Vervoort, J. D., and Patchett, P. J., 2008, The Lu–Hf and Sm–Nd isotopic composition of CHUR: constraints from unequilibrated chondrites and implications for the bulk composition of terrestrial planets.: Earth Planet. Sci. Lett. , v. 273, p. 48–57.

Cleveland, W. S., 1979, Robust locally weighted fitting and smoothing scatterplots: Journal of the American Statistical Association, v. 74, p. 829-836.

Fisher, C. M., Vervoort, J. D., and DuFrane, S. A., 2014, Accurate Hf isotope determinations of complex zircons using the "laser ablation split stream" method: Geochemistry, Geophysics, Geosystems, v. 15, no. 1, p. 121-139.

Foster, G., 1996, Wavelets for period analysis of unevenly sampled time series: The Astronomical Journal v. 112, p. 1709-1729.

Gardiner, N. J., Hickman, A. H., Kirkland, C. L., Lu, Y., Johnson, T., and Zhao, J.-X., 2017, Processes of crust formation in the early Earth imaged through Hf isotopes from the East Pilbara Terrane: Precambrian Research, v. 297, p. 56-76.

Gardiner, N. J., Kirkland, C. L., and Van Kranendonk, M. J., 2016, The Juvenile Hafnium Isotope Signal as a Record of Supercontinent Cycles: Scientific Reports, v. 6.

Gardiner, N. J., Mulder, J. A., Kirkland, C. L., Johnson, T. E., and Nebel, O., 2021, Palaeoarchaean TTGs of the Pilbara and Kaapvaal cratons compared; an early Vaalbara supercraton evaluated: South African Journal of Geology, v. 124, no. 1, p. 37-52.

Gardiner, N. J., Wacey, D., Kirkland, C. L., Johnson, T. E., and Jeon, H., 2019, Zircon U-Pb, Lu-Hf and O isotopes from the 3414 Ma Strelley Pool Formation, East Pilbara Terrane and the Palaeoarchaean emergence of a cryptic cratonic core: Precambrian Research, v. 321, p. 64-84.

Gillman, M., and Erenler, H., 2019, Reconciling the Earth's stratigraphic record with the structure of our galaxy: Geoscience Frontiers, v. 10, no. 6, p. 2147-2151.

Glikson, A. Y., and Pirajno, F., 2018, Asteroids Impacts, Crustal Evolution and Related Mineral Systems with Special Reference to Australia, Springer, Modern Approaches in Solid Earth Sciences.

Griffin, W., Pearson, N., Belousova, E., Jackson, S., O'Reilly, S., van Achterberg, E., and Shee, S., 2000, The Hf isotope composition of cratonic mantle: LAM-MC-ICPMS analysis of zircon megacrysts in kimberlites: Geochimica et Cosmochimica Acta, v. 64, p. 133–147.

Griffin, W., Wang, X., Jackson, S., Pearson, N., O'Reilly, S., Xu, X., and Zhou, X., 2002a, Zircon chemistry and magma genesis, SE China: in-situ analysis of Hf isotopes, Pingtan and Tonglu igneous complexes: Lithos, v. 61, p. 237–269.

Griffin, W. L., Wang, X., Jackson, S. E., Pearson, N. J., O'Reilly, S. Y., Xu, X., and Zhou, X., 2002b, Zircon chemistry and magma mixing, SE China: In-situ analysis of Hf isotopes, Tonglu and Pingtan igneous complexes: Lithos, v. 61, no. 3, p. 237-269.

Geological Suvery of Western Australia, 2020, Compilation of geochronology information, 2020, Department of Mines, Industry, Resources, Safety, digital data package. http://www.dmp.wa.gov.au/geochron/

Hammer, Ø., Harper, D. A. T., and Ryan, P. D., 2001, PAST: Paleontological Statistics Software Package for Education and Data Analysis.: Palaeontologia Electronica, v. 4, p. 9.

Johnson, T. E., Kirkland, C. L., Lu, Y., Smithies, R. H., Brown, M., and Hartnady, M., 2022, Giant impacts and the origin and evolution of continents: Nature, in press. 10.1038/s41586-022-04956-y

Junqueira, T. C., Lépine, J. R. D., Braga, C. A. S., and Barros, D. A., 2013, A new model for gravitational potential perturbations in disks of spiral galaxies. An application to our Galaxy: A&A, v. 550.

Kemp, A. I. S., Hickman, A. H., Kirkland, C. L., and Vervoort, J. D., 2015, Hf isotopes in detrital and inherited zircons of the Pilbara Craton provide no evidence for Hadean continents: Precambrian Research, v. 261, p. 112-126.

Kirkland, C. L., Yakymchuk, C., Hollis, J., Heide-Jørgensen, H., and Danišík, M., 2018, Mesoarchean exhumation of the Akia terrane and a common Neoarchean tectonothermal history for West Greenland: Precambrian Research, v. 314, p. 129-144.

Lieberman, B. S., and Melott, A. L., 2007, Considering the case for biodiversity cycles: re-examining the evidence for periodicity in the fossil record.: PLoS One, v. 2, no. 8, p. e759.

Lu, Y., Wingate, M.T.D., Smithies, R.H., Martin, L., Jeon, H., Champion, D.C., Johnson, S.P. and Mole, D.R., 2021, Zircon oxygen isotope map of Western Australia: Geological Survey of Western Australia, digital data layer.

Melott, A. L., and Bambach, R. K., 2011, A ubiquitous~ 62-Myr periodic fluctuation superimposed on general trends in fossil biodiversity. I. Documentation: Paleobiology, v. 37, no. 1, p. 92-112.

Morel, M. L. A., Nebel, O., Nebel-Jacobsen, Y. J., Miller, J. S., and Vroon, P. Z., 2008, Hafnium isotope characterization of the GJ-1 zircon reference material by solution and laser-ablation MC-ICPMS. : Chemical Geology, v. 255, p. 231-235.

Olierook, H. K. H., Kirkland, C. L., Hollis, J. A., Gardiner, N. J., Yakymchuk, C., Szilas, K., Hartnady, M. I. H., Barham, M., McDonald, B. J., Evans, N. J., Steenfelt, A., and Waterton, P., 2021, Regional zircon U-Pb geochronology for the Maniitsoq region, southwest Greenland: Scientific Data, v. 8, no. 1, p. 139.

Petersson, A., Kemp, A. I. S., Gray, C. M., and Whitehouse, M. J., 2020, Formation of early Archean Granite-Greenstone Terranes from a globally chondritic mantle: Insights from igneous rocks of the Pilbara Craton, Western Australia: Chemical Geology, v. 551, p. 119757.

Petersson, A., Kemp, A. I. S., Hickman, A. H., Whitehouse, M. J., Martin, L., and Gray, C. M., 2019a, A new 3.59 Ga magmatic suite and a chondritic source to the east Pilbara Craton: Chemical Geology, v. 511, p. 51–70.

Petersson, A., Kemp, A. I. S., and Whitehouse, M. J., 2019b, A Yilgarn seed to the Pilbara Craton (Australia)? Evidence from inherited zircons: Geology, v. 47, p. 1098–1102.

Pidgeon, R. T., Nemchin, A. A., and Cliff, J., 2013, Interaction of weathering solutions with oxygen and U–Pb isotopic systems of radiation-damaged zircon from an Archean granite, Darling Range Batholith, Western Australia: Contributions to Mineralogy and Petrology, v. 166, no. 2, p. 511-523.

Rohde, R. A., and Muller, R. A., 2005, Cycles in fossil diversity: Nature, v. 434, no. 7030, p. 208-210.

Sanchez-Blazquez, P., Courty, S., Gibson, B. K., and Brook, C. B., 2009, The origin of the light distribution in spiral galaxies. : Monthly Notices of the Royal Astronomical Society, v. 398, no. 2, p. 591-606.

Schulz, M., and Mudelsee, M., 2002, REDFIT: estimating red-noise spectra directly from unevenly spaced paleoclimatic time series. : Computers & Geosciences, v. 28, p. 421-426.

Smithies, R. H., Lu, Y., Kirkland, C. L., Johnson, T. E., Mole, D. R., Champion, D. C., Martin, L., Jeon, H., Wingate, M. T. D., and Johnson, S. P., 2021, Oxygen isotopes trace the origins of Earth's earliest continental crust: Nature, v. 592, no. 7852, p. 70-75.

Söderlund, U., Patchett, P. J., Vervoort, J. D., and Isachsen, C. E., 2004, The 176Lu decay constant determined by Lu–Hf and U–Pb isotope systematics of Precambrian mafic intrusions. : Earth Planet. Sci. Lett., v. 219, p. 311-324.

Thirlwall, M. F., and Anczkiewicz, R., 2004, Multidynamic isotope ratio analysis using MC–ICP–MS and the causes of secular drift in Hf, Nd and Pb isotope ratios. : Int. J. Mass Spectrom., v. 235, p. 59-81.

Torrence, C., and Compo, G. P., 1998, A practical guide to wavelet analysis.: Bulletin of the American Meteorological Society v. 79, p. 61-78.

Vallée, J. P., 2017, A guided map to the spiral arms in the galactic disk of the Milky Way.: Astronomical Review, v. 13, no. 3-4, p. 113-146.

Woodhead, J., Hergt, J., Shelley, M., Eggins, S., and Kemp, R., 2004, Zircon Hf-isotope analysis with an excimer laser, depth profiling, ablation of complex geometries, and concomitant age estimation.: Chemical Geology, v. 209, p. 121-135.

Zeileis, A., and Grothendieck, G., 2005, zoo: S3 Infrastructure for Regular and Irregular Time Series: Journal of Statistical Software; Vol 1, Issue 6.